Individual and interactive effects of warming and CO_2 on *Pseudo-nitzschia subcurvata* and *Phaeocystis antarctica*, two dominant phytoplankton from the Ross Sea, Antarctica

Zhi Zhu[1], Pingping Qu[1], Jasmine Gale[1], Feixue Fu[1], David A. Hutchins[1]

1. Department of Biological Science, University of Southern California, Los Angeles, CA 90089, USA.

Correspondence to: David A. Hutchins (dahutch@usc.edu)

Abstract: We investigated the effects of temperature and CO_2 variation on the growth and elemental composition of cultures of the diatom *Pseudo-nitzschia subcurvata* and the prymnesiophyte *Phaeocystis antarctica,* two ecologically dominant phytoplankton species isolated from the Ross Sea, Antarctica. To obtain thermal functional response curves, cultures were grown across a range of temperatures from 0^oC to 14^oC. In addition, a co-culturing experiment examined the relative abundance of both species at 0^oC and 6^oC. CO_2 functional response curves were conducted from 100 to 1730 ppm at 2^oC and 8^oC to test for interactive effects between the two variables. The growth of both phytoplankton was significantly affected by temperature increase, but with different trends. Growth rates of *P. subcurvata* increased with temperature from 0°C to maximum levels at 8°C, while the growth rates of *P. antarctica* only increased from 0°C to 2°C. The maximum thermal limits of *P. subcurvata* and *P. antarctica* where growth stopped completely were 14°C and 10°C, respectively. Although *P. subcurvata* outgrew *P. antarctica* at both temperatures in the co-incubation experiment, this happened much faster at 6°C than at 0°C. For *P. subcurvata,* there was a significant interactive effect in which the warmer temperature decreased the CO_2 half saturation constant for growth, but this was not the case for *P. antarctica*. The growth rates of both species increased with CO_2 increases up to 425 ppm, and in contrast to significant effects of temperature, the effects of CO_2 increase on their elemental composition were minimal. Our results suggest that future warming may be more

1 Introduction

Global temperature is predicted to increase 2.6°C to 4.8°C by 2100 with increasing anthropogenic CO_2 emissions (IPCC, 2014). The temperature of the Southern Ocean has increased even faster than global average temperature (Meredith and King, 2005), and predicted future climate warming may profoundly change the ocean carbon cycle in this region (Sarmiento et al., 1998). The Ross Sea, Antarctica, is one of the most productive area in the ocean, and features annual austral spring and summer algal blooms dominated by *Phaeocystis* and diatoms that contribute as much as 30% of total primary production in the Southern Ocean (Arrigo et al., 1999, 2008; Smith et al., 2000, 2014a). The responses of phytoplankton in the Ross Sea to future temperature change (Rose et al., 2009; Xu et al., 2014; Zhu et al., 2016) in combination with intensified stratification (Sarmiento et al., 1998) could lead to intensified future diatom blooms (Smith et al. 2014b), and the physiological effects of warming may partially compensate for a lack of iron throughout much of this region (Hutchins and Boyd, 2016).

In the Ross Sea, the colonial prymnesiophyte *Phaeocystis antarctica* typically blooms in austral spring and early summer, and diatoms including *Pseudo-nitzschia subcurvata* and *Chaetoceros* spp. bloom later in the austral summer (Arrigo et al., 1999, 2000; DiTullio and Smith, 1996; Goffart et al., 2000; Rose et al., 2009). Both diatoms and *P. antarctica* play an important role in anthropogenic CO_2 drawdown and the global carbon cycle; additionally, they contribute significantly to the global silicon and sulfur cycles, respectively (Arrigo et al., 1999; Tréguer et al., 1995; Schoemann et al., 2005). Furthermore, the N: P and C: P ratios of *P. antarctica* are higher than those of diatoms, and thus they contribute unequally to the carbon, nitrogen, and phosphorus cycles (Arrigo et al., 1999, 2000). Diatoms are preferred by many planktonic herbivores over *P. antarctica,* and so the two groups also differentially influence the food webs of the Southern Ocean (Knox, 1994; Caron et al., 2000; Haberman et al., 2003).

Arrigo et al. (1999) suggested that the spatial and temporal distributions of *P. antarctica*

dominant groups of phytoplankton. Smith and Jones (2015) presented evidence for the importance of deep mixing and the critical depth for the timing of transitions from *P. antarctica* to diatom blooms. Zhu et al. (2016) observed that a 4ºC temperature increase promoted the growth rates of several dominant diatoms isolated from Ross Sea, including *P. subcurvata*, *Chaetoceros* sp., and *Fragilariopsis cylindrus*, but not the growth rates of *P. antarctica*. In addition, both field and laboratory research has suggested that temperature increase and iron addition can synergistically promote the growth of Ross Sea diatoms (Rose et al., 2009; Zhu et al., 2016; Hutchins and Boyd, 2016). Thus, it is possible that phytoplankton community structure in this region may change in the future under a global warming scenario.

In addition to temperature increases, ocean uptake of 30% of total emitted anthropogenic CO_2 has led to a 0.1 pH unit decrease in surface water, corresponding to a 26% increase in acidity (IPCC, 2014). The global CO_2 concentration is predicted to increase to around 800 ppm by 2100, which will lead to a further decrease in surface seawater pH of 0.3–0.4 units (Orr et al., 2005; IPCC, 2014). CO_2 increases have been found to promote the growth and affect the physiology of many but not all phytoplankton species tested (Fu et al., 2007, 2008; King et al., 2011; Xu et al., 2014; Hutchins and Fu 2017).

Research on the effects of CO_2 increases on *Phaeocystis antarctica* and Antarctic diatoms is still scarce. Xu et al. (2014) suggested that future conditions (higher temperature, CO_2, and irradiance) may shift phytoplankton community structure towards diatoms and away from *P. antarctica* in the Ross Sea. Trimborn et al. (2013) discovered that the growth rates of *P. antarctica* and *P. subcurvata* were not significantly promoted by high CO_2 relative to ambient CO_2 at 3°C. In contrast, Wang et al. (2010) observed that the growth rates of the closely related temperate colonial species *Phaeocystis globosa* increased significantly at 750 ppm CO_2 relative to 380 ppm CO_2.

Many studies have shown that primary production in various parts of the Southern Ocean

and warming on the growth of phytoplankton from the Ross Sea (Rose et al., 2009; Zhu et al., 2016; Hutchins and Boyd 2016). Thus, an important goal of phytoplankton research is to also gain an understanding of how global warming together with ocean acidification may shift the phytoplankton community in the Ross Sea (Arrigo et al., 1999; DiTullio et al., 2000). This study aimed to explore the effects of increases in temperature and CO_2 availability, both individually and in combination, on *P. antarctica* and *P. subcurvata* isolated from the Ross Sea, Antarctica. These results may shed light on the potential effects of global change on the marine ecosystem and the cycles of carbon and nutrients in the highly productive coastal polynyas of Antarctica.

2 Materials and Methods

2.1 Strains and growth conditions

P. subcurvata and *P. antarctica* were isolated from the ice edge in McMurdo Sound (77.62° S, 165.47° E) in the Ross Sea, Antarctica during January 2015; *P. antarctica* cultures grew as small colonies (~4-12 cells) in all the experiments. All stock cultures were grown in Aquil* medium (100 µmol L^{-1} NO_3^-, 100 µmol L^{-1} SiO_4^{4-},10 µmol L^{-1} PO_4^{3-}) made with 0.2 µM-filtered seawater that was collected from the same Ross Sea locale as the culture isolates (Sunda et al., 2005). Stock and experimental cultures were grown in Fe-replete Aquil medium (0.5 µM). Although phytoplankton in the open Ross Sea polynya are generally proximately iron-limited (Ryan-Keogh et al. 2017), these culture conditions are relevant to the coastal McMurdo Sound ice edge environment in the early spring when Fe is relatively abundant, and typically not limiting. This 'winter reserve' iron is then drawn down in this nearshore environment over the course of the seasonal algal bloom to eventually reach limiting levels (Sedwick et al., 2011; Bertrand et al., 2015). Our experiments address warming and acidification responses in *P. subcurvata* and *P. antarctica* in the absence of any differential effects of Fe availability; interactive effects of Fe limitation with warming and/or acidification in these two species are

111 For thermal functional response curves, experimental cultures of both phytoplankton
112 were grown in triplicate 500 ml acid washed polycarbonate bottles and gradually acclimated by a
113 series of step-wise transfers to a range of temperatures, including 0°C, 2°C, 4°C, 6°C, 8°C, and
114 10°C (*P. antarctica* died at 10°C) under the same light cycle as stock cultures. Cultures were
115 diluted semi-continuously following Zhu et al. (2016). All of the cultures were acclimated to
116 their respective temperatures for 8 weeks before the commencement of the experiment. At this
117 point, after the growth rates were verified to be stable for at least three to five consecutive
118 transfers, the cultures were sampled 48 h after dilution (Zhu et al., 2016).
119 For CO_2 functional response curves, *P. antarctica* and *P. subcurvata* were also grown in
120 triplicate in a series of six CO_2 concentrations from ~100 ppm to ~1730 ppm in triplicate 500 ml
121 acid washed polycarbonate bottles at both 2°C and 8°C using same dilution technique as above.
122 The CO_2 concentration was achieved by gently bubbling with 0.2 μm filtered air/CO_2 mixture
123 (Gilmore, CA) and carbonate system equilibration was ensured by pH and dissolved inorganic
124 carbon (DIC) measurements (King et al., 2015, see below).
125 An additional experiment tested whether temperature-related trends in growth rates
126 observed in monocultures were maintained when both species were grown together in a simple
127 model community. For this examination of thermal effects on the growth of *P. antarctica* and *P.*
128 *subcurvata* in co-culture (pre-acclimated to respective temperatures), the isolates were mixed at
129 equal Chl *a* (chlorophyll *a*) concentrations and grown together for 6 days in triplicate bottles at
130 both 0°C and 6°C. These temperatures chosen to span the optimum growth ranges of both
131 species (see Results, below). The relative abundance of each phytoplankton was then calculated
132 based on cell counts taken on days 0, 3 and 6.
133 **2.3 Growth rates**
134 Cell count samples were counted on a Sedgewick Rafter Grid using an Olympus BX51
135 microscope before and after dilution for each treatment. Samples that couldn't be counted

$$\mu = (\ln N_1 - \ln N_0)/t, \quad (1)$$

where N_0 and N_1 are the cell density at the beginning and end of a dilution period, respectively, and t is the duration of the dilution period (Zhu et al. 2016). The Q_{10} of growth rates was calculated following Chaui-Berlinck et al. (2002) as Eq. (2):

$$Q_{10} = (\mu_2/ \mu_1)^{10/(T_2-T_1)}, \quad (2)$$

where μ_1 and μ_2 are the specific growth rates of the phytoplankton at temperatures T_1 and T_2, respectively. The growth rates were fitted to Eq. (3) to estimate the thermal reaction norms of each species:

$$f(T) = ae^{bT}(1- ((T-z)/(w/2))^2), \quad (3)$$

where specific growth rate *f* depends on temperature (T), temperature niche width (*w*), and other empirical parameters *z, a*, and *b* were estimated by maximum likelihood (Thomas et al., 2012; Boyd et al., 2013). Afterwards, the optimum temperature for growth and maximum growth rate were estimated by numerically maximizing the equation (Boyd et al., 2013). The growth rates of all the species at all the CO_2 levels were fitted to Michaelis-Menten equation as Eq. (4):

$$\mu = \mu_{max} S/(K_m + S), \quad (4)$$

to estimate maximum growth rates (μ_{max}) and half saturation constants (K_m) for CO_2 concentration (S). In the CO_2 curve experiments growth rates for both these autotrophic species were assumed to be zero at 0 ppm CO_2, and in the thermal curve experiments growth rates were assumed to be zero at -2°C, approximately the freezing point of seawater.

2.4 Elemental and Chl *a* analysis

Culture samples for particulate organic carbon/nitrogen (POC/PON) and particulate organic phosphorus (POP) analyses were filtered onto pre-combusted (500°C for 2 h) GF/F filters and dried at 60°C overnight. A 30 ml aliquot of *P. subcurvata* culture for each treatment were filtered onto 2 μm polycarbonate filters (GE Healthcare, CA) and dried in a 60°C oven overnight for biogenic silica (BSi) analysis. The analysis method of POC/PON and POP

-20°C for 24 h for Chl *a* analysis. The Chl *a* concentration was then determined using the non-acidification method on a 10-AU^{TM} fluorometer (Turner Design, CA) (Fu et al., 2007).

2.5 pH and dissolved inorganic carbon (DIC) measurements

pH was measured using a pH meter (Thermo Scientific, MA), calibrated with pH 7 and 10 buffer solutions. For DIC analyses, an aliquot of 25 mL was preserved with 200 μL 5% $HgCl_2$ and stored in the dark at 4^{o}C until analysis. Total DIC was measured using a CM140 Total Inorganic Carbon Analyzer (UIC Inc., IL). An aliquot of 5 mL sample was injected into the sparging column of Acidification Unit CM5230 (UIC Inc., IL) followed by 2 ml 10% phosphoric acid. By using flow rates controlled pure nitrogen as carrier gas, and the CO_2 released from the DIC pool in the sample was quantified with a CM5015 CO_2 Coulometer (UIC Inc., IL) using absolute coulometric titration. The carbonate buffer system was sampled for each of the triplicate bottles in each treatment at the beginning and end of the experiments; reported values are final ones. The pCO_2 in growth media was calculated using CO2SYS (Pierrot et al., 2006). These carbonate system measurements are shown in Table 1, along with the corresponding calculated pCO_2 values calculated. Kinetic parameters were calculated using the individual calculated pCO_2 values for each replicate (see above), but for convenience, the CO_2 treatments are referred to in the text using the mean value of all experimental bottles, rounded to the nearest 5 ppm: these values are 100 ppm, 205 ppm, 260 ppm, 425 ppm, 755 ppm, and 1730 ppm.

2.6 Statistical analysis

All statistical analyses and model fitting, including student t-tests, ANOVA, Tukey's HSD test, two-way ANOVA, and thermal reaction norms estimation were conducted using the open source statistical software R version 3.1.2 (R Foundation).

3 Results

3.1 Temperature effects on growth rates

Temperature increase significantly affected the growth rates of both *P. antarctica* and *P.*

192 0.05) (Fig. 1). The growth rates of *P. antarctica* significantly increased from 0°C to 2°C, and
193 plateaued at 4°C and 6°C, and then significantly decreased from 6°C to 8°C ($p < 0.05$) (Fig. 1).
194 *P. antarctica* and *P. subcurvata* stopped growing at 10°C and 14°C, respectively (Fig. 1A). The
195 specific growth rates of *P. subcurvata* were not significantly different from those of *P. antarctica*
196 at 0°C, 2°C and 4°C, but became significantly higher than *P. antarctica* at 6°C, and remained
197 significantly higher than *P. antarctica* through 8°C and 10°C ($p < 0.05$) (Fig. 1A). The optimum
198 temperatures for growth of *P. antarctica* and *P. subcurvata* were 4.85°C and 7.36°C,
199 respectively, both well above the current temperature in the Ross Sea, Antarctica (Table 2). In
200 addition, the estimated temperature niche width of *P. subcurvata* (-2°C – 12.19°C) is wider than
201 that of *P. antarctica* (-2.0°C to 9.52°C) (Table 2); calculated minimum temperatures estimated
202 from the thermal niche width equation were less than -2.0°, the freezing point of seawater, and so
203 growth is assumed to terminate at -2.0°. The Q10 value of the growth rate of *P. antarctica* from
204 0°C to 4°C is 2.11, which is lower than the Q10 values 3.17 for *P. subcurvata* over the same
205 temperature interval ($p < 0.05$) (Table 2).

206 **3.2 Temperature effects on elemental composition**

207 The C: N and N: P ratios of *P. subcurvata* were unaffected by changing temperature (Fig.
208 2A, B), but the C: P, C: Si, and C: Chl *a* ratios of this species were significantly affected ($p <$
209 0.05) (Fig. 2C, D, Fig. 3). The C: P ratios of *P. subcurvata* were slightly but significantly lower
210 in the middle of the tested temperature range. They were higher at 8°C and 10°C than at 2°C,
211 4°C, and 6°C ($p < 0.05$) (Fig. 2C), and also significantly higher at 10°C than at 0°C (Fig. 2C).
212 The C: Si ratios of *P. subcurvata* showed a similar pattern of slightly lower values at mid-range
213 temperatures; at 0°C and 2°C they were significantly higher than at 6°C and 8°C ($p < 0.05$) (Fig.
214 2D), and significantly higher at 2°C and 10°C than at 4°C and 8°C, respectively (Fig. 2D). The
215 C: Chl *a* ratios of *P. subcurvata* also showed this trend of somewhat lower values in the middle
216 of the thermal gradient. At 0°C, 8°C and 10°C, C: Chl *a* ratios were significantly higher than at

The C: N, N: P, C: P, and C: Chl *a* ratios of *P. antarctica* were not significantly different across the temperature range (Fig. 2A, B, C, Fig. 3). The N: P ratios of *P. antarctica* were significantly higher than those of *P. subcurvata* at 2°C, 6°C, and 8°C ($p < 0.05$) (Fig. 2B). Additionally, the C: P ratios of *P. antarctica* were significantly higher than those of *P. subcurvata* at 6°C and 8°C ($p < 0.05$) (Fig. 2C), and the C: Chl *a* ratios of *P. antarctica* were significantly higher than values of *P. subcurvata* at all the temperatures tested ($p < 0.05$) (Fig. 3).

Temperature change significantly affected the cellular carbon (C) quotas, cellular nitrogen (N) quotas, cellular phosphorus (P) quotas, cellular silica (Si) quotas, and cellular Chl *a* quotas of *P. subcurvata* ($p < 0.05$) (Table 3). The cellular C and N quotas of *P. subcurvata* were significantly higher at 8°C than at 0°C ($p < 0.05$) (Table 3), the cellular P quotas of *P. subcurvata* were significantly higher at 4°C than at 0°C, 2°C, and 10°C ($p < 0.05$) (Table 3), and the cellular Si quotas of *P. subcurvata* were significantly higher at 8°C than at 0°C and 2°C. Si quotas were also significantly higher at 4°C and 6°C than at 0°C ($p < 0.05$) (Table 3). The extreme temperatures significantly decreased the cellular Chl *a* quotas of *P. subcurvata*, as the cellular Chl *a* quotas of this species were significantly higher at 4°C, 6°C, and 8°C than at 0°C and 10°C ($p < 0.05$) (Table 3).

Temperature change significantly affected the cellular P quotas and cellular Chl *a* quotas of *P. antarctica* ($p < 0.05$), but not the cellular C and N quotas ($p > 0.05$) (Table 3). The cellular P quotas of *P. antarctica* were significantly higher at 0°C than at 8°C ($p < 0.05$) (Table 3), and the Chl *a* quotas of the prymnesiophyte were significantly lower at 8°C than at 0°C, 2°C, and 6°C ($p < 0.05$) (Table 3).

3.3 Co-incubation at two temperatures

A warmer temperature favored the dominance of *P.subcurvata* over *P. antarctica* in the model community experiment. Although *P. subcurvata* increased its abundance relative to the prymnesiophyte at both temperatures by day 6, this increase was larger and happened much

The carbonate system was relatively stable across the range of CO_2 levels during the course of the experiment (Table 1). CO_2 concentration significantly affected the growth rates of *P. subcurvata* at both temperatures (Fig. 5). The growth rates of the diatom at 2°C increased steadily with CO_2 concentration increase from 205 ppm to 425 ppm ($p < 0.05$), but were saturated at 755 ppm and 1730 ppm (Fig. 5A). Similarly, the growth rates of *P. subcurvata* at 8°C increased with CO_2 concentration increase from 205 ppm to 260 ppm ($p < 0.05$), and were saturated at 425 ppm, 755 ppm and 1730 ppm (Fig. 5B). The growth rates of the diatom at all CO_2 concentrations tested at 8°C were significantly higher than at 2°C ($p < 0.05$); for instance, the maximum growth rate of *P. subcurvata* at 8°C was 0.88 d^{-1}, significantly higher than the value of 0.60 d^{-1} at 2°C ($p < 0.0.5$) (Table 4). In addition, the pCO_2 half saturation constant (K_m) of *P. subcurvata* at 8°C was 10.7 ppm, significantly lower than 66.0 ppm at 2°C ($p < 0.0.5$) (Table 4). Thus, temperature and CO_2 concentration increase interactively increased the growth rates of *P. subcurvata* ($p < 0.05$).

CO_2 concentration also significantly affected the growth rates of *P. antarctica* at both 2°C and 8°C. The growth rates of the prymnesiophyte at both 2°C and 8°C increased with CO_2 concentration increase from 100 ppm to 260 ppm ($p < 0.05$), and were saturated at 425 ppm and 755 ppm (Fig. 5C, D). The growth rates of *P. antarctica* at 2°C decreased slightly at 1730 ppm relative to 425 ppm and 755 ppm ($p < 0.05$) (Fig. 5C). The maximum growth rate of *P. antarctica* at 8°C was 0.43 d^{-1}, significantly lower than the value of 0.61 d^{-1} at 2°C ($p < 0.05$) (Table 4). The pCO_2 half saturation constants of *P. antarctica* at 2°C and 8°C were not significantly different (Table 4), and thus no interactive effect of temperature and CO_2 was observed on the growth rate of the prymnesiophyte ($p > 0.05$).

3.5 CO_2 effects on elemental composition at two temperatures

CO_2 concentration variation didn't affect the C: N, N: P, or C: P ratios of *P. subcurvata* at either 2°C or 8°C. The C: Si ratios of *P. subcurvata* were significantly higher at 1730 ppm

ppm ($p < 0.05$) (Table 5). The C: P ratios of *P. subcurvata* at 8°C were significantly higher than at 2°C at all the CO_2 levels tested ($p < 0.05$) (Table 5). The C: Si ratios of *P. subcurvata* at CO_2 levels lower than 755 ppm at 8°C were significantly lower than at 2°C ($p < 0.05$) (Table 5). The higher temperature also significantly increased the C: Chl *a* ratios of *P. subcurvata* at all the CO_2 levels tested ($p < 0.05$) (Table 5). Additionally, the temperature increase and CO_2 concentration increase interactively decreased the C: Chl *a* ratios of *P. subcurvata* ($p < 0.05$) (Table 5).

The CO_2 concentration increase did not affect the C: N, N: P, and C: P ratios of *P. antarctica* at either 2°C or 8°C. The carbon to Chl *a* ratios of *P. antarctica* were significantly higher at 1730 ppm than at all lower CO_2 concentrations at 2°C. Similarly, at 8°C the carbon to Chl *a* ratios of this species also were significantly higher at 425 ppm, 755 ppm, and 1730 ppm than at lower CO_2 concentrations ($p < 0.05$) (Table 5), and significantly higher at 1730 ppm than at 425 ppm and 755 ppm ($p < 0.05$) (Table 5).

The warmer temperature significantly decreased the C: N ratios of *P. antarctica* at 260 ppm and 755 ppm CO_2 ($p < 0.05$) (Table 5), and C: P ratios also decreased at 100 ppm and 205 ppm($p < 0.05$) (Table 5). The C: Chl *a* ratios of *P. antarctica* at CO_2 levels higher than 205 ppm were significantly higher at 8°C relative to 2°C ($p < 0.05$) (Table 5). Temperature and CO_2 concentration increase interactively increased the C: Chl *a* ratios of *P. antarctica* ($p < 0.05$) (Table 5).

The CO_2 concentration increase didn't affect the cellular C, N, P, or Si quotas of *P. subcurvata* at 2°C, or the C quotas and N quotas at 8°C. The Si quotas of *P. subcurvata* were significantly lower at 1730 ppm CO_2 than at 100 ppm and 205 ppm at 8°C ($p < 0.05$) (Table 6). The cellular Chl *a* quotas of *P. subcurvata* were significantly lower at 8°C relative to 2°C at CO_2 higher than 205 ppm ($p < 0.05$) (Table 6). The temperature increase significantly increased the cellular Si quota of *P. subcurvata* at all the CO_2 levels tested except 1730 ppm ($p < 0.05$) (Table 6). Additionally, warming and CO_2 concentration interactively decreased the cellular Si quotas of

The C, N, and P quotas of *P. antarctica* were not affected by CO_2 increase at 2°C, and N and P quotas were not affected by CO_2 increase at 8°C, either. However, the C quota of *P. antarctica* at 1730 ppm CO_2 was significantly higher than CO_2 levels lower than 755 ppm at 8°C ($p < 0.05$) (Table 6). The Chl *a* per cell of *P. antarctica* at 1730 ppm CO_2 was significantly less than at lower CO_2 levels at both 2°C and 8°C ($p < 0.05$) (Table 6). For *P. antarctica*, the Chl *a* per cell values at 100 ppm, 205 ppm, and 755 ppm CO_2 at 8°C were significantly lower relative to 2°C ($p < 0.05$) (Table 6). Temperature increase and CO_2 concentration increase interactively increased the C and N quotas of *P. antarctica* ($p < 0.05$) (Table 6).

4 Discussion

As has been documented in previous work, the diatom *P. subcurvata* and the prymnesiophyte *P. antarctica* responded differently to warming (Xu et al., 2014; Zhu et al. 2016). In the Ross Sea as elsewhere, temperature determines both phytoplankton maximum growth rates (Bissinger et al., 2008) and the upper limit of growth (Smith, 1990) in a species-specific manner. Thermal functional responses curves of phytoplankton typically increase in a normally distributed pattern, with growth rates increasing up to the optimum temperature range, and then declining when temperature reaches inhibitory levels (Boyd et al., 2013; Fu et al., 2014; Xu et al., 2014; Hutchins and Fu, 2017). Specific growth rates of *P. subcurvata* reached optimal levels at 8°C, demonstrating that this species grows fastest at temperatures substantially above any temperatures found in the present-day Ross Sea. In contrast, growth rates of *P. antarctica* saturated at 2°C. Zhu et al. (2016) found that 4°C warming significantly promoted the growth rates of *P. subcurvata* but not *P. antarctica*. Xu et al. (2014) found that the growth rates of another strain of *P. antarctica* (CCMP3314) decreased in a multi-variable "year 2100 cluster" condition (6°C, 81 Pa CO_2, 150 μmol photons m^{-2} s^{-1}) relative to the "current condition" (2°C, 39 Pa CO_2, and 50 μmol photons m^{-2} s^{-1}) and the "year 2060 condition" (4°C, 61 Pa CO_2, and 100 μmol photons m^{-2} s^{-1}). In our study, the Q10 value of *P. subcurvata* from 0°C to 4°C was

al. (2016). Our results showed that the maximal thermal limit of *P. antarctica* was reached at 10°C, as was also observed by Buma et al. (1991), while *P. subcurvata* did not cease to grow until 14°C. Clearly, *P. subcurvata* has a superior tolerance to higher temperature compared to *P. antarctica*.

The co-incubation experiment with *P. subcurvata* and *P. antarctica* at 0°C and 6°C confirmed that the diatom retained its growth advantage at the higher temperature when growing together with *P. antarctica*. Although we do not know what role (if any) competition for resources like nutrients may have played in determining the outcome of this experiment, it did demonstrate clearly that thermal growth response trends in simple model communities are consistent with those seen in unialgal cultures. Xu el al. (2014) observed that the diatom *Fragilariopsis cylindrus* was dominant over *P. antarctica* under "year 2060 conditions" (4°C, 61 Pa CO_2, and 100 μmol photons m^{-2} s^{-1}). These experiments support the results of a Ross Sea field survey which suggested that water temperature structured the phytoplankton assemblage (Liu and Smith, 2012), and may shed light on why *P. antarctica* is often dominant in cooler waters in the springtime, while diatoms often dominate in summer (DiTullio and Smith, 1996; Arrigo et al., 1999; DiTullio et al., 2000; Liu and Smith, 2012).

Besides temperature, mixed layer depth and irradiance also likely play a role in the competition between diatoms and *P. antarctica* (Arrigo et al., 1999; Arrigo et al., 2010, Smith and Jones 2015). Arrigo et al. (1999) observed that *P. antarctica* dominated the southern Ross Sea region with deeper mixed layers, while diatom dominated the regions with shallower mixed layer depths. The niches of these two groups of phytoplankton are difficult to define by either light or by temperature, since shallow surface stratification tends to promote both solar heating and high irradiance, while deep mixing often lowers both light and temperatures. It is worth considering whether these two phytoplankton groups are each best adapted to a different environmental matrix of both variables. This concept of different light/temperature niches for

Temperature change affected the C: P, N: P and C: Si ratios of *P. subcurvata*, due to the combined effects of the different responses of cellular C, P, and Si quotas. The C: P and N:P ratios of *P. subcurvata* increased at the two highest temperatures tested. This might be due to an increase in protein translation efficiency and a corresponding decrease in phosphate-rich ribosomes with warming, which can result in a decreased cellular P requirement per unit of carbon in marine phytoplankton (Toseland et al., 2013). Similarly lowered P quotas at higher temperatures have been documented in other studies as well (Xu et al., 2014; Boyd et al., 2015; Hutchins and Boyd, 2016). This result suggests that the amount of carbon exported per unit phosphorus by *P. subcurvata* (and perhaps other diatoms) in the Ross Sea may increase as temperature increases in the future (Toseland et al., 2013).

In contrast, the decreasing trend of C: Si ratios in *P. subcurvata* appears to be largely due to higher cellular Si quotas at temperatures at and above 4°C. Although the physiological reason(s) for increased silicification with warming are currently not understood, this trend also may have biogeochemical consequences. This decrease of cellular C: Si ratios at higher temperature may tend to enhance Si export, with the qualification that biogenic Si remineralization rates also increase with temperature (Ragueneau et al. 2000), and thus could potentially offset this trend.

Previous studies have shown that nutrient drawdown by diatoms and *P. antarctica* are different, due to differing elemental ratios of these two groups (Arrigo et al., 1999; Smith et al., 2014a; Xu et al., 2014). Our results generally corresponded to this trend, as the N: P ratios of *P. antarctica* were higher than *P. subcurvata* at 2°C, 6°C and 8°C and C: P ratios of *P. antarctica* were higher than *P. subcurvata* at 6°C and 8°C ($p < 0.05$) (Fig. 2). Although elemental ratios of the prymnesiophyte were largely unaffected by temperature, a predicted increase of diatom and decrease of *P. antarctica* contributions to phytoplankton production caused by warming will likely change nutrient export ratios (Smith et al., 2014a, b). It is possible that N and C export per

Our results showed that the growth rates of both *P. subcurvata* and *P. antarctica* exhibited moderate limitation by CO_2 levels lower than ~425 ppm at both 2°C and 8°C; this observation is significant, since during the intense Ross Sea summertime phytoplankton bloom pCO_2 can sometimes drop to very low levels (Tagliabue and Arrigo, 2016). However, at CO_2 concentrations beyond current atmospheric levels of ~400 ppm, growth rates of *P. subcurvata* or *P. antarctica* were CO_2-saturated. Although a general model prediction suggests that an atmospheric CO_2 increase from current levels to 700 ppm could increase the growth of marine phytoplankton by 40% (Schippers et al., 2004), our results instead correspond to previous studies which showed negligible effects of elevated CO_2 on various groups of phytoplankton (Goldman, 1999; Fu et al., 2007; Hutchins and Fu 2017). In particular, Trimborn et al. (2013) found that increasing CO_2 had no effect on growth rates of Southern Ocean isolates of *P. subcurvata* and *P. antarctica*. The minimal effects of changing CO_2 levels on many phytoplankton groups have been suggested to be due to efficient carbon concentrating mechanisms (CCMs) that allow them to avoid CO_2 limitation at low pCO_2 levels (Burkhardt et al., 2001; Fu et al., 2007; Tortell et al., 2008). For instance, both *P. subcurvata* and *P. antarctica* have been shown to strongly downregulate activity of the important CCM enzyme carbonic anhydrase as CO_2 increases (Trimborn et al. 2013). Clearly, though, for our two species their CCM activity was not sufficient to completely compensate for carbon limitation at low pCO_2 levels. Although speculative, it is possible that *P. antarctica* could have an ability to subsidize growth at very low CO_2 levels through oxidation of organic carbon from the colony mucilage. Our results also showed that very high CO_2 (1730 ppm) significantly reduced the growth rate of *P. antarctica* relative to 425 ppm and 755 ppm at 2°C; negative effects of high CO_2 on an Antarctic microbial community were also observed by Davidson et al. (2016). This inhibitory effect might be due to the significantly lower pH at 1730 ppm (~7.4), which could entail expenditures of additional energy to maintain pH homeostasis within cells.

405 growth was much lower at the warmer temperature. In contrast, warming decreased the maximal
406 growth rates of *P. antarctica* over the range of CO_2 concentrations tested, and failed to change its
407 $K_{1/2}$ for growth. The decreased CO_2 $K_{1/2}$ of *P. subcurvata* at high temperature might confer a
408 future additional competitive advantage over *P. antarctica* in the late growing season when pCO_2
409 can be low (Tagliabue and Arrigo, 2016) and temperatures higher, although temperatures are
410 generally never as high as 8°C in the current Ross Sea (Liu and Smith, 2012). The CO_2 $K_{1/2}$ of *P.*
411 *antarctica* at 2°C was however significantly lower than that of *P. subcurvata* at this temperature,
412 which may be advantageous to the prymnesiophyte when water temperatures are low in the
413 spring.

414 The effects of pCO_2 variation on the elemental ratios of *P. subcurvata* and *P. antarctica*
415 were minimal relative to those of temperature increase. Previous research on the effects of CO_2
416 on the elemental ratios of phytoplankton has shown that the elemental composition of
417 phytoplankton may change with CO_2 availability (Burkhardt et al., 1999; Fu et al., 2007, 2008;
418 Tew et al., 2014; reviewed in Hutchins et al., 2009). Hoogstraten et al. (2012) found that CO_2
419 concentration change didn't change the cellular POC, PON, C: N ratios, or POC to Chl *a* ratios
420 of the temperate species *Phaeocystis globosa*. In contrast, Reinfelder (2014) observed that the N
421 and P quotas of several diatoms decreased with increasing CO_2 and led to increased C: N, N: P,
422 and C: P ratios. King et al. (2015) found that high CO_2 could increase, decrease or not affect the
423 C: P and N: P ratios of several different phytoplankton species. Our results resemble those of
424 studies with other phytoplankton that found that the effects of CO_2 concentration can be
425 negligible on C: N, N: P, or C: P ratios (Fu et al., 2007; Hutchins et al., 2009; Hoogstraten et al.,
426 2012; King et al., 2015).

427 In contrast to C: N: P ratios, we observed that the C: Si ratios of *P. subcurvata* were
428 significantly higher at 1730 ppm compared to almost all of the lower CO_2 levels. This increase in
429 C: Si ratios was due to a decrease in cellular Si quotas at 1730 ppm CO_2. Milligan et al. (2004)

toxic diatom *Pseudo-nitzschia fraudulenta*, in which cellular C: Si ratios were higher at 765 ppm than at 200 ppm CO_2. This suggests that future increases in diatom silicification at elevated pCO_2 could partially or wholly offset the decreased silicification and higher dissolution rates of silica observed at warmer temperatures (above); to fully predict net trends, further interactive experiments focusing on silicification as a function across a range of both temperature and pCO_2 are needed.

In conclusion, our results indicate that *P. subcurvata* from the Ross Sea are better adapted to higher temperature than is *P. antarctica*. Diatoms are a diverse group, but if their general thermal response is similar to that of this *Pseudo-nitzschia* species, they may thrive under future global warming scenarios while the relative dominance of *P. antarctica* in this region may wane. In contrast, another recent study has suggested that warming might indirectly favor *P. antarctica* springtime dominance by leading to large areas of open water at a time when incident light penetration is low and mixed layers are still relatively deep (Ryan-Keogh et al. 2017). Because of the differences in elemental ratios in the two groups, ecological shifts that favor diatoms may significantly increase the export of phosphorus and silicon relative to carbon and nitrogen, while increased *P. antarctica* dominance will increase carbon export relative to nutrient fluxes, as well as enhancing the organic sulfur cycle. Our conclusions must be qualified as they were obtained using Fe-replete culture conditions, similar to conditions often found early in the growing season in McMurdo Sound. However, Fe limitation generally prevails later in the season here, and elsewhere in the offshore Ross Sea. Irradiance is an additional key environmental factor to consider in both the present and future in this region (Smith and Jones, 2015). Thus, in addition to warming and CO_2 increases, the interactive effects of light and Fe with these two factors should also be considered (Xu et al., 2014; Boyd et al., 2015; Hutchins and Boyd 2016; Hutchins and Fu 2017). Considering the differences between the responses of the diatom and *P. antarctica* to warming and ocean acidification seen here, as well to warming and Fe in previous work (Zhu

production in the Ross Sea polynya may need to realistically incorporate a complex network of interacting global change variables.

Author contribution

Z. Zhu, F. X. Fu, D. A. Hutchins designed the experiments, Z. Zhu, P. Qu, and J. Gale carried them out, and Z. Zhu and D. A. Hutchins wrote the manuscripts.

Competing interests

The authors declare that they have no conflict of interest.

Acknowledgments

We want to thank Kai Xu for isolating all these phytoplankton strains. Support for this research was provided by National Science Foundation grant ANT 1043748 to D. A. Hutchins

References

Arrigo, K. R., Robinson, D. H., Worthen, D. L., Dunbar, R. B., DiTullio, G. R., VanWoert, M., and Lizotte, M. P.: Phytoplankton community structure and the drawdown of nutrients and CO_2 in the Southern Ocean, Science, 283, 365-367, 1999.

Arrigo K. R., DiTullio G. R., Dunbar R. B., Robinson D. H., Van Woert M., Worthen D. L., Lizotte M. P.: Phytoplankton taxonomic variability in nutrient utilization and primary production in the Ross Sea, J. Geophys Res: Oceans, 105, 8827-8846, 2000.

Arrigo, K. R., van Dijken, G. L., and Bushinsky, S.: Primary production in the Southern Ocean, 1997–2006, J. Geophys Res, 113, C08004, doi:10.1029/2007JC004551, 2008.

Arrigo, K. R., Mills, M. M., Kropuenske, L. R., van Dijken, G. L., Alderkamp, A. C., and Robinson, D. H.: Photophysiology in two major Southern Ocean phytoplankton taxa: photosynthesis and growth of *Phaeocystis antarctica* and *Fragilariopsis cylindrus* under different irradiance levels, Integrative and Comparative Biology, 50(6), 950-966, 2010.

Bertrand, E.M., McCrow, J.P., Zheng, H., Moustafa, A., McQuaid, J., Delmont, T., Post, A.,

484 bacterial interactions mediate micronutrient colimitation in the Southern Ocean, P. Natl. Acad.
485 Sci. USA, 112. doi:10.1073/pnas.1501615112, 2015.
486 Bissinger, J. E., Montagnes, D. J., Sharples, J., and Atkinson, D.: Predicting marine
487 phytoplankton maximum growth rates from temperature: Improving on the Eppley curve using
488 quantile regression, Limnol. Oceanogr., 53, 487, 2008.
489 Boyd, P. W., Rynearson, T. A., Armstrong, E. A., Fu, F., Hayashi, K., Hu, Z., Hutchins, D.A.,
490 Kudela, R.M., Litchman, E., Mulholland, M.R. and Passow, U.: Marine phytoplankton
491 temperature versus growth responses from polar to tropical waters–outcome of a scientific
492 community-wide study, PLoS One, 8, available at:
493 http://dx.doi.org/10.1371/journal.pone.0063091, 2013.
494 Boyd, P. W., Dillingham, P. W., McGraw, C. M., Armstrong, E. A., Cornwall, C. E., Feng, Y.
495 Y., Hurd, C.L., Gault-Ringold, M., Roleda, M.Y., Timmins-Schiffman, E. and Nunn, B. L.:
496 Physiological responses of a Southern Ocean diatom to complex future ocean conditions, Nature
497 Climate Change, 6, 207-213, 2015.
498 Boyd, P. W., Watson, A. J., Law, C. S., Abraham, E. R., Trull, T., Murdoch, R., Bakker, D. C.,
499 Bowie, A. R., Buesseler, K. O., Chang, H., and Charette, M.: A mesoscale phytoplankton bloom
500 in the polar Southern Ocean stimulated by iron fertilization, Nature, 407(6805): 695-702, 2000.
501 Buma, A. G. J., Bano, N., Veldhuis, M. J. W., and Kraay, G. W.: Comparison of the
502 pigmentation of two strains of the prymnesiophyte *Phaeocystis* sp., Neth. J. Sea Res., 27(2), 173-
503 182, 1991.
504 Burkhardt, S., Zondervan, I., and Riebesell, U.: Effect of CO_2 concentration on C: N: P ratio in
505 marine phytoplankton: A species comparison, Limnol. Oceanogr., 44, 683-690, 1999.
506 Burkhardt, S., Amoroso, G., Riebesell, U., and Sültemeyer, D.: CO_2 and HCO_3^{-1} uptake in
507 marine diatoms acclimated to different CO_2 concentrations, Limnol. Oceanogr., 46, 1378-1391,
508 2001.

511 3272, 2000.
512 Chaui-Berlinck, J. G., Monteiro, L. H. A., Navas, C. A., and Bicudo, J. E. P.: Temperature
513 effects on energy metabolism: a dynamic system analysis, P. Roy. Soc. Lond. B Bio., 269, 15-19,
514 2002.
515 Coale, K. H., Johnson, K. S., Chavez, F. P., Buesseler, K. O., Barber, R. T., Brzezinski, M. A.,
516 Cochlan, W. P., Millero, F. J., Falkowski, P. G., Bauer, J. E., and Wanninkhof, R. H.: Southern
517 Ocean iron enrichment experiment: carbon cycling in high-and low-Si waters, Science,
518 304(5669), 408-414, 2004.
519 Davidson, A. T., McKinlay, J., Westwood, K., Thompson, P. G., van den Enden, R., de Salas,
520 M., Wright, S., Johnson, R., and Berry, K.: Enhanced CO_2 concentrations change the structure of
521 Antarctic marine microbial communities, Mar. Ecol-Prog. Ser., 552, 92-113, 2016.
522 DiTullio, G. R., and Smith, W. O.: Spatial patterns in phytoplankton biomass and pigment
523 distributions in the Ross Sea. J. Geophys Res: Oceans, 101, 18467-18477, 1996.
524 DiTullio, G. R., Grebmeier, J. M., Arrigo, K. R., Lizotte, M. P., Robinson, D. H., Leventer, A.,
525 Barry, J.P., VanWoert, M.L. and Dunbar, R. B.: Rapid and early export of *Phaeocystis*
526 *antarctica* blooms in the Ross Sea, Antarctica, Nature, 404, 595-598, 2000.
527 El-Sabaawi, R., and Harrison, P. J.: Interactive effects of irradiance and temperature on the
528 photosynthetic physiology of the pennate diatom *Pseudo-nitzschia Granii* (Bacillariophyceae)
529 from the northeast Subarctic Pacific, J. Phycol., 42, 778-785, 2006.
530 Fabry, V. J. (2008). Marine calcifiers in a high-CO_2 ocean. *Science*, 320(5879), 1020-1022.
531 Fu, F. X., Warner, M. E., Zhang, Y., Feng, Y., and Hutchins, D. A.: Effects of increased
532 temperature and CO_2 on photosynthesis, growth, and elemental ratios in marine *Synechococcus*
533 and *Prochlorococcus* (cyanobacteria), J. Phycol., 43, 485-496, 2007.
534 Fu, F. X., Zhang, Y., Warner, M. E., Feng, Y., Sun, J., and Hutchins, D. A.: A comparison of
535 future increased CO_2 and temperature effects on sympatric *Heterosigma akashiwo* and

537 Fu, F. X., Yu, E., Garcia, N. S., Gale, J., Luo, Y., Webb, E. A., and Hutchins, D. A.: Differing
538 responses of marine N_2 fixers to warming and consequences for future diazotroph community
539 structure, Aquat. Microb. Ecol., 72, 33-46, 2014.
540 Gille, S. T.: Warming of the Southern Ocean since the 1950s, Science, 295, 1275-1277, 2002.
541 Goldman, J. C.: Inorganic carbon availability and the growth of large marine diatoms, Mar. Ecol-
542 Prog. Ser., 180, 81-91, 1999.
543 Haberman, K. L., Ross, R. M., and Quetin, L. B.: Diet of the Antarctic krill (Euphausia superba
544 Dana): II. Selective grazing in mixed phytoplankton assemblages, J. Exper. Mar. Biol.
545 Ecol., 283, 97-113, 2003.
546 Hoogstraten, A., Peters, M., Timmermans, K. R., and De Baar, H. J. W.: Combined effects of
547 inorganic carbon and light on *Phaeocystis globosa* Scherffel
548 (Prymnesiophyceae), Biogeosciences, 9, 1885-1896, 2012.
549 Hutchins, D.A., Mulholland, M.R. and Fu, F. X.: Nutrient cycles and marine microbes in a CO_2-
550 enriched ocean, Oceanography, 22, 128-145, 2009.
551 Hutchins, D.A. and Boyd, P.W.: Marine phytoplankton and the changing ocean iron cycle,
552 Nature Climate Change, 6, 1071-1079, 2016.
553 Hutchins, D. A., and Fu, F. X.: Microorganisms and ocean global change. *Nature Microbiology*,
554 In press, 2017.
555 Hutchins, D. A., Sedwick, P. N., DiTullio, G. R., Boyd, P. W., Queguiner, B., Griffiths, F. B.,
556 and Crossley, C.: Control of phytoplankton growth by iron and silicic acid availability in the
557 subantarctic Southern Ocean: Experimental results from the SAZ Project, J. Geophys. Res.
558 Oceans, 106(C12), 31559-31572, 2001.
559 IPCC, 2014: Climate Change 2014: Impacts, Adaptation, and Vulnerability. Part A: Global and
560 Sectoral Aspects. Contribution of Working Group II to the Fifth Assessment Report of the
561 Intergovernmental Panel on Climate Change.

562 King, A. L., Sanudo-Wilhelmy, S. A., Leblanc, K., Hutchins, D. A., and Fu, F. X.: CO_2 and
563 vitamin B12 interactions determine bioactive trace metal requirements of a subarctic Pacific
564 diatom, The ISME J., 5, 1388-1396, 2011.
565 King, A. L., Jenkins, B. D., Wallace, J. R., Liu, Y., Wikfors, G. H., Milke, L. M., and Meseck, S.
566 L.: Effects of CO_2 on growth rate, C: N: P, and fatty acid composition of seven marine
567 phytoplankton species, Mar. Ecol-Prog. Ser., 537, 59-69, 2015.
568 Knox, G. A.: The Biology of the Southern Ocean, Cambridge University Press, New York, USA,
569 1994.
570 Liu, X., and Smith, W. O.: Physiochemical controls on phytoplankton distributions in the Ross
571 Sea, Antarctica, J. Marine Syst., 94, 135-144, 2012.
572 Martin, J. H., Gordon, R. M., and Fitzwater, S. E.: Iron in Antarctic waters, Nature, 345(6271),
573 156-158, 1990.
574 Meredith, M. P., and King, J. C.: Rapid climate change in the ocean west of the Antarctic
575 Peninsula during the second half of the 20th century, Geophys. Res. Lett., 32, L19604,
576 doi:10.1029/2005GL024042, 2005.
577 Milligan, A. J., Varela, D. E., Brzezinski, M. A., and Morel, F. M.: Dynamics of silicon
578 metabolism and silicon isotopic discrimination in a marine diatom as a function of
579 pCO_2, Limnol. Oceanogr, 49, 322-329, 2004.
580 Orr, J. C., Fabry, V. J., Aumont, O., Bopp, L., Doney, S. C., Feely, R. A., Gnanadesikan, A.,
581 Gruber, N., Ishida, A., Joos, F. and Key, R. M.: Anthropogenic ocean acidification over the
582 twenty-first century and its impact on calcifying organisms, Nature, 437, 681-686, 2005.
583 Paasche, E.: Silicon and the ecology of marine plankton diatoms. II. Silicate-uptake kinetics in
584 five diatom species, Mar. Biol., 19, 262-269, 1973.
585 Ragueneau, O., Tréguer, P., Leynaert, A., Anderson, R. F., Brzezinski, M. A., DeMaster, D. J.,
586 Fischer, G., Francois, R., and Heinze, C.: A review of the Si cycle in the modern ocean: recent

589 Reinfelder, J. R.: Carbon dioxide regulation of nitrogen and phosphorus in four species of marine
590 phytoplankton, Mar. Ecol-Prog. Ser., 466, 57-67, 2012.
591 Pierrot, D., Lewis, E., and Wallace, D. W. R.: MS Excel program developed for CO_2 system
592 calculations. ORNL/CDIAC-105a. Carbon Dioxide Information Analysis Center, Oak Ridge
593 National Laboratory, US Department of Energy, Oak Ridge, Tennessee, 2006.
594 Rose, J. M., Feng, Y., DiTullio, G. R., Dunbar, R. B., Hare, C. E., Lee, P. A., Lohan, M.C.,
595 Long, M.C., Smith, W.O., Sohst, B.M., and Tozzi, S.: Synergistic effects of iron and temperature
596 on Antarctic phytoplankton and microzooplankton assemblages, Biogeosciences, 6, 3131-3147,
597 2009.
598 Ryan-Keogh, T. J., DeLizo, L. M., Smith, W. O. Jr., Smith, Sedwick, P. N., McGillicuddy, D. J.,
599 Jr.. Moore, C. M., and Bibby, T. S. Temporal progression of photosynthetic-strategy in
600 phytoplankton in the Ross Sea, Antarctica, J. Mar. Sys., 166, 87-96,
601 DOI:10.1016/j.jmarsys.2016.08.014, 2017.
602 Sarmiento, J. L., Hughes, T. M., Stouffer, R. J., and Manabe, S.: Simulated response of the ocean
603 carbon cycle to anthropogenic climate warming, Nature, 393, 245-249, 1998.
604 Schippers, P., Lürling, M., and Scheffer, M.: Increase of atmospheric CO_2 promotes
605 phytoplankton productivity, Ecol. Lett, 7, 446-451, 2004.
606 Schoemann V., Becquevort S., Stefels J., Rousseau V., Lancelot C.: *Phaeocystis* blooms in the
607 global ocean and their controlling mechanisms: a review, J. Sea Res., 53, 43-66, 2005.
608 In: Smith, W. O.: Polar Oceanography, Chemistry, Biology and Geology, Academic Press,
609 Massachusetts, USA, 1990.
610 Sedwick, P. N., DiTullio, G. R., and Mackey, D. J.: Iron and manganese in the Ross Sea,
611 Antarctica: Seasonal iron limitation in Antarctic shelf waters, J. Geophys. Res.: Oceans,
612 105(C5), 11321-11336, 2000.
613 Sedwick, P. N., Marsay, C. M., Sohst, B. M., Aguilar-Islas, A. M., Lohan, M. C., Long, M. C.

616 Antarctic continental shelf. J. Geophys. Res.: Oceans, 116: C12019, DOI:
617 10.1029/2010JC006553, 2011.
618 Smith, W. O., Ainley, D. G., Arrigo, K. R., and Dinniman, M. S.: The oceanography and ecology
619 of the Ross Sea. Annual Review of Marine Science, 6, 469-487, 2014a.
620 Smith, W. O., Dinniman, M. S., Hofmann, E. E., and Klinck, J. M.: The effects of changing
621 winds and temperatures on the oceanography of the Ross Sea in the 21st century. GeophyS. Res.
622 Lett., 41, 1624-1631, 2014b.
623 Smith, W.O., Jr., and Jones, R.M.: Vertical mixing, critical depths, and phytoplankton growth in
624 the Ross Sea. ICES J. Mar. Sci., 72, 6, 1952-1960, 2015.
625 Smith, W. O., Marra, J., Hiscock, M. R., and Barber, R. T.: The seasonal cycle of phytoplankton
626 biomass and primary productivity in the Ross Sea, Antarctica, Deep-Sea Res. Pt. II, 47, 3119-
627 3140, 2000.
628 Takeda S.: Influence of iron availability on nutrient consumption ratio of diatoms in oceanic
629 waters, Nature, 393(6687), 774-777, 1998.
630 Tagliabue, A., and Arrigo, K.R.: Decadal trends in air-sea CO_2 exchange in the Ross Sea
631 (Antarctica), Geophys. Res. Lett., 43, 5271-5278, 2016.
632 Tatters, A.O., Fu, F.X. and Hutchins, D.A.: High CO_2 and silicate limitation synergistically
633 increase the toxicity of *Pseudo-nitzshia fraudulenta*, PLoS ONE, 7, available at:
634 http://dx.doi.org/10.1371/journal.pone.0032116, 2012.
635 Tew, K. S., Kao, Y. C., Ko, F. C., Kuo, J., Meng, P. J., Liu, P. J., and Glover, D. C.: Effects of
636 elevated CO_2 and temperature on the growth, elemental composition, and cell size of two marine
637 diatoms: potential implications of global climate change, Hydrobiologia, 741, 79-87, 2014.
638 Thomas, M. K., Kremer, C. T., Klausmeier, C. A., and Litchman, E.: A global pattern of thermal
639 adaptation in marine phytoplankton, Science, 338, 1085-1088, 2012.
640 Tortell, P. D., Payne, C., Gueguen, C., Li, Y., Strzepek, R. F., Boyd, P. W., and Rost, B.: Uptake

643 Toseland, A. D. S. J., Daines, S. J., Clark, J. R., Kirkham, A., Strauss, J., Uhlig, C., Lenton,
644 T.M., Valentin, K., Pearson, G.A., Moulton, V. and Mock, T. (2013). The impact of temperature
645 on marine phytoplankton resource allocation and metabolism. Nature Climate Change, 3(11),
646 979-984.
647 Treguer, P., Nelson, D. M., Van Bennekom, A. J., and DeMaster, D. J.: The silica balance in the
648 world ocean: a reestimate, Science, 268, 375, 1995.
649 Trimborn, S., Brenneis, T., Sweet, E., and Rost, B.: Sensitivity of Antarctic phytoplankton
650 species to ocean acidification: Growth, carbon acquisition, and species interaction, Limnol.
651 Oceanogr., 58, 997-1007, 2013.
652 Wang, Y., Smith, W. O., Wang, X., and Li, S.: Subtle biological responses to increased CO_2
653 concentrations by *Phaeocystis globosa* Scherffel, a harmful algal bloom species, Geophys. Res.
654 Lett., 37, L09604, doi:10.1029/2010GL042666, 2010.
655 Xu, K., Fu, F. X., and Hutchins, D. A.: Comparative responses of two dominant Antarctic
656 phytoplankton taxa to interactions between ocean acidification, warming, irradiance, and iron
657 availability, Limnol. Oceanogr., 59, 1919-1931, 2014.
658 Zhu, Z., Xu, K., Fu, F., Spackeen, J. L., Bronk, D. A., and Hutchins, D. A.: A comparative study
659 of iron and temperature interactive effects on diatoms and *Phaeocystis antarctica* from the Ross
660 Sea, Antarctica, Mar. Ecol-Prog. Ser., 550, 39-51, 2016.
661

Table 1. The measured pH and dissolved inorganic carbon (DIC), and calculated pCO_2 of *P. subcurvata* and *P. antarctica* at 2°C and 8°C in each treatment. Values represent the means and errors are the standard deviations of triplicate bottles.

P. subcurvata		*P. antarctica*	
2°C	8°C	2°C	8°C
pH			
8.36±0.04	8.51±0.04	8.40±0.03	8.45±0.03
8.25±0.04	8.36±0.01	8.22±0.04	8.29±0.01
8.07±0.01	8.17±0.01	8.09±0.02	8.14±0.00
7.86±0.02	7.99±0.01	7.85±0.01	7.94±0.00
7.68±0.01	7.79±0.02	7.65±0.01	7.75±0.00
7.35±0.01	7.46±0.02	7.34±0.01	7.45±0.00
DIC (μmol/kg)			
1890.1±26.6	1846.5±15.8	1847.1±30.0	1831.1±22.7
2049.1±10.8	1985.7±2.1	2033.9±15.0	2014.2±19.9
2131.3±9.4	2067.5±4.7	2136.6±5.6	2085.3±15.3
2190.4±2.8	2156.1±13.9	2168.1±12.4	2167.4±21.5
2260.0±22.2	2234.8±10.3	2252.1±11.5	2238.7±12.0
2340.1±19.4	2334.5±18.8	2338.2±12.1	2323.7±11.5
pCO_2 (ppm)			
109.1±9.3	94.4±10.1	96.6±9.5	108.8±8.8
158.6±15.5	150.3±3.6	171.2±14.4	183.6±4.2
263.1±5.9	254.2±9.9	246.4±9.9	280.3±0.6
450.2±17.3	414.9±12.0	462.2±12.1	480.9±4.7
740.9±10.6	708.8±23.5	786.9±10.3	784.1±4.8
1751.2±35.9	1675.3±49.4	1769.9±59.5	1720.3±18.3

669 Table 2. Statistical comparison of the results for each of the three thermal traits: Optimum temperature

670 (ºC), Maximum growth rate (d^{-1}) and temperature niche width (W)* of *P. subcurvata* and *P. antarctica.*

671

Species	Optimum temperature (ºC)	Maximum growth rates (d^{-1})	W upper CI	W lower CI	Q_{10}
P. subcurvata	7.36	0.86	12.19	< -2.0	3.17
P. antarctica	4.85	0.66	9.52	< -2.0	2.11

672

673 * The statistical results for the lower bound of temperate niche width in both species were lower
674 than -2.0ºC, the freezing point of seawater
675

676 Table 3. The effects of temperature on the C quota (pmol cell^{-1}), N quota (pmol cell^{-1}), P quota (pmol
677 cell^{-1}), Si quota (pmol cell^{-1}), and chl *a* per cell (pg cell^{-1}) of *P. subcurvata* and *P. antarctica.* Values
678 represent the means and errors are the standard deviations of triplicate bottles.
679

	P. subcurvata	*P. antarctica*
C quota		
0°C	1.91±0.14	2.64±0.34
2°C	2.11±0.19	2.49±0.41
4°C	2.15±0.12	2.50±0.23
6°C	2.07±0.13	2.26±0.18
8°C	2.33±0.14	2.17±0.22
10°C	2.17±0.13	
N quota		
0°C	0.27±0.03	0.39±0.03
2°C	0.29±0.03	0.36±0.02
4°C	0.33±0.02	0.40±0.01
6°C	0.31±0.01	0.35±0.02
8°C	0.36±0.05	0.34±0.03
10°C	0.33±0.04	
P quota		
0°C	0.02±0.00	0.03±0.00
2°C	0.02±0.00	0.02±0.00
4°C	0.03±0.00	0.03±0.01
6°C	0.03±0.00	0.02±0.00
8°C	0.03±0.00	0.02±0.00
10°C	0.02±0.00	
Si quota		
0°C	0.23±0.02	
2°C	0.23±0.06	
4°C	0.30±0.01	
6°C	0.30±0.03	
8°C	0.34±0.01	
10°C	0.28±0.04	
Chl a per cell (pg/cell)		
0°C	0.48±0.01	0.23±0.03
2°C	0.57±0.07	0.22±0.02
4°C	0.64±0.01	0.20±0.01
6°C	0.68±0.05	0.21±0.00
8°C	0.58±0.03	0.17±0.02
10°C	0.46±0.03	

680
681
682

683 Table 4. Comparison of the curve fitting results for maximum growth rate (d^{-1}) and half saturation

684 constants (K_m), calculated from the CO_2 functional response curves of *P. subcurvata* and *P. antarctica* at

685 2°C and 8°C. Values represent the means and errors are the standard errors from fitting.

686 .

Species	Maximum growth rates (d^{-1})	K_m
P. subcurvata		
2°C	0.60±0.18	66.4±10.39
8°C	0.88±0.02	9.8±5.34
P. antarctica		
2°C	0.61±0.02	26.4±8.23
8°C	0.41±0.02	22.1±11.15

687

Table 5 The effects of CO_2 on the C: N, N: P, C: P, C: Si, and C: Chl *a* ratios of *P. subcurvata* and *P. antarctica* at 2°C and 8°C. Values represent the means and errors are the standard deviations of triplicate bottles.

	P. subcurvata		*P. antarctica*	
	2°C	8°C	2°C	8°C
C: N				
100 ppm	6.6±0.26	7.1±0.68	7.22±0.50	6.95±0.35
205 ppm	6.7±0.24	7.5±0.32	7.74±0.21	6.56±1.15
260 ppm	6.7±0.32	7.3±0.18	8.07±0.52	6.99±0.27
425 ppm	6.7±0.05	6.6±0.05	7.21±0.81	6.19±0.13
755 ppm	6.8±0.20	7.1±0.68	7.98±0.44	6.79±0.22
1730 ppm	7.1±0.82	7.4±1.07	8.15±0.48	7.05±0.91
N: P				
100 ppm	10.4±0.85	14.5±2.28	16.4±1.24	13.9±0.20
205 ppm	10.8±1.01	13.3±0.42	16.6±1.12	15.7±2.77
260 ppm	10.3±1.28	14.0±0.56	14.3±1.24	14.5±2.38
425 ppm	11.3±0.84	16.5±0.28	17.1±1.83	17.2±1.98
755 ppm	9.9±0.28	14.3±1.34	14.2±2.60	11.6±4.11
1730 ppm	10.4±1.02	15.5±1.84	15.5±0.56	15.1±1.85
C: P				
100 ppm	68.6±3.10	101.0±6.43	117.7±4.08	96.7±4.86
205 ppm	72.7±4.82	99.3±7.05	128.2±5.98	101.0±1.91
260 ppm	69.1±7.68	103.0±4.88	115.5±7.25	101.0±13.04
425 ppm	76.3±5.19	109.0±2.20	122.3±4.85	106.0±11.14
755 ppm	67.2±1.38	101.0±5.80	113.5±22.50	78.6±27.09
1730 ppm	73.4±1.22	114.0±5.99	126.2±12.10	105.0±6.26
C: Si				
100 ppm	7.8±0.80	5.6±0.32		
205 ppm	7.4±0.30	5.6±0.24		
260 ppm	7.3±0.23	6.1±0.38		
425 ppm	7.5±0.23	6.1±0.06		
755 ppm	7.4±0.66	6.3±0.36		
1730 ppm	8.0±0.88	7.1±0.47		
C: Chl *a* (μg/μg)				
100 ppm	43.6±1.14	70.7±5.01	160.4±6.68	197.4±29.35
205 ppm	45.2±2.91	67.3±4.42	157.5±4.95	194.0±17.14
260 ppm	41.6±3.31	60.1±9.45	138.3±15.19	169.8±9.20
425 ppm	37.2±2.58	72.5±2.35	180.2±20.10	232.4±20.47
755 ppm	42.2±3.62	68.7±6.29	167.5±5.06	282.5±15.30
1730 ppm	46.3±2.23	85.3±15.70	276.5±36.57	460.3±15.21

698 Table 6 The effects of CO_2 on the C quota (pmol cell^{-1}), N quota (pmol cell^{-1}), P quota (pmol cell^{-1}), Si

699 quota (pmol cell^{-1}), and chl *a* per cell (pg cell^{-1}) of *P. subcurvata* and *P. antarctica* at 2°C and 8°C.

700 Values represent the means and errors are the standard deviations of triplicate bottles.

	P. subcurvata		*P. antarctica*	
	2°C	8°C	2°C	8°C
C quota				
100 ppm	2.0±0.15	2.64±0.06	2.57±0.03	2.15±0.22
205 ppm	2.1±0.12	2.67±0.31	2.72±0.28	2.35±0.19
260 ppm	1.9±0.04	2.28±0.18	2.51±0.36	2.21±0.04
425 ppm	1.8±0.04	2.43±0.15	2.31±0.05	2.28±0.46
755 ppm	2.1±0.09	2.26±0.05	2.47±0.17	2.81±0.15
1730 ppm	2.1±0.30	2.47±0.18	2.43±0.10	2.96±0.30
N quota				
100 ppm	0.30±0.03	0.38±0.04	0.36±0.03	0.31±0.03
205 ppm	0.30±0.03	0.36±0.03	0.35±0.03	0.36±0.06
260 ppm	0.29±0.01	0.31±0.02	0.31±0.06	0.32±0.02
425 ppm	0.27±0.01	0.37±0.06	0.32±0.03	0.37±0.05
755 ppm	0.30±0.02	0.32±0.03	0.31±0.03	0.41±0.01
1730 ppm	0.29±0.05	0.34±0.06	0.30±0.03	0.43±0.10
P quota				
100 ppm	0.03±0.00	0.03±0.00	0.02±0.00	0.02±0.00
205 ppm	0.03±0.00	0.03±0.00	0.02±0.00	0.02±0.00
260 ppm	0.03±0.00	0.02±0.00	0.02±0.00	0.02±0.00
425 ppm	0.02±0.00	0.02±0.00	0.02±0.00	0.02±0.01
755 ppm	0.03±0.00	0.02±0.00	0.02±0.00	0.04±0.02
1730 ppm	0.03±0.00	0.02±0.00	0.02±0.00	0.03±0.00
Si quota				
100 ppm	0.26±0.02	0.47±0.04		
205 ppm	0.28±0.02	0.48±0.07		
260 ppm	0.27±0.01	0.37±0.03		
425 ppm	0.25±0.01	0.40±0.04		
755 ppm	0.28±0.03	0.36±0.03		
1730 ppm	0.26±0.01	0.35±0.05		
Chl a per cell (pg/cell)				
100 ppm	0.54±0.05	0.45±0.04	0.19±0.01	0.13±0.02
205 ppm	0.54±0.04	0.48±0.05	0.21±0.02	0.15±0.02
260 ppm	0.56±0.03	0.46±0.04	0.22±0.04	0.16±0.01
425 ppm	0.60±0.04	0.40±0.04	0.16±0.02	0.12±0.01
755 ppm	0.59±0.06	0.40±0.03	0.18±0.01	0.12±0.00
1730 ppm	0.53±0.06	0.35±0.05	0.11±0.02	0.08±0.01

701
702
703

Figure legends

Fig. 1. Thermal functional response curves showing specific growth rates (and fitted curves) of *Pseudo-nitzschia subcurvata* and *Phaeocystis antarctica* across a range of temperatures from 0°C to 14°C. Values represent the means and error bars represents the standard deviations of triplicate samples.

Fig. 2. The C: N ratios (A), N: P ratios (B), and C: P ratios (C) of *Pseudo-nitzschia subcurvata* and *Phaeocystis antarctica* and (D) the C: Si ratios of *Pseudo-nitzschia subcurvata* from the thermal response curves shown in Fig. 1 for a range of temperatures from 0°C to 10°C. Values represent the means and error bars represents the standard deviations of triplicate samples.

Fig. 3. The C: Chl *a* ratios of *Pseudo-nitzschia subcurvata* and *Phaeocystis antarctica* from the thermal response curves shown in Fig. 1 for a range of temperatures from 0°C to 10°C. Values represent the means and error bars represents the standard deviations of triplicate samples.

.

Fig. 4. The relative abundance of *Pseudo-nitzschia subcurvata* in a 6 day competition experiment with *Phaeocystis antarctica* at 0°C and 6°C. The competition experiments were started with equal Chl *a* concentrations for both species, and the relative abundance was calculated based on cell counts. Values represent the means and error bars represents the standard deviations of triplicate samples.

Fig. 5. CO_2 functional response curves showing specific growth rates (and fitted curves) across a range of CO_2 concentrations from ~100 ppm to ~1730 ppm at 2°C and at 8°C. *Pseudo-nitzschia subcurvata* at 2°C (A) and 8°C (B) and *Phaeocystis antarctica* at 2°C (C) and 8°C (D). Values

Fig. 1

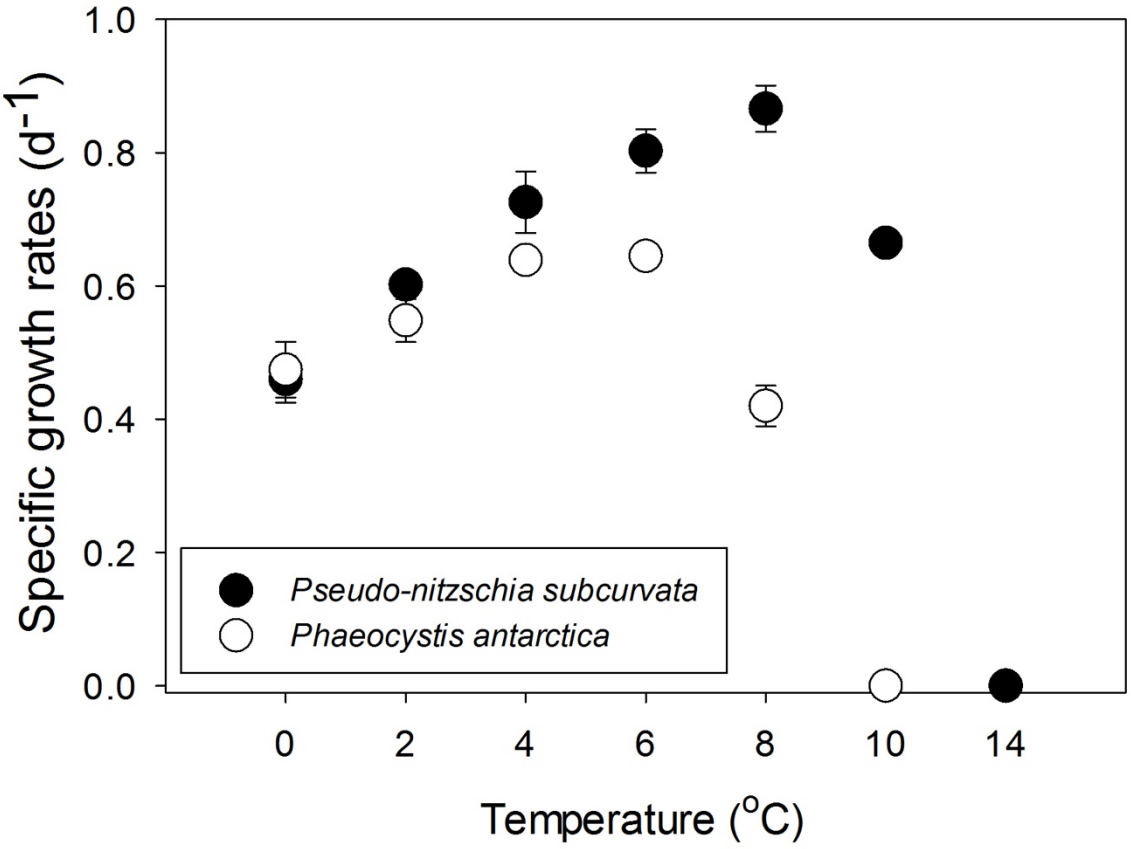
Specific growth rates (d-1)
1.0
0.8
0.6
0.4
0.2
0.0
0
2
4
6
8
10
14
Temperature (°C)
Pseudo-nitzschia subcurvata
Phaeocystis antarctica

763 Fig. 2
764
765
766
767
768
769
770
771
772
773
774
775
776
777
778
779

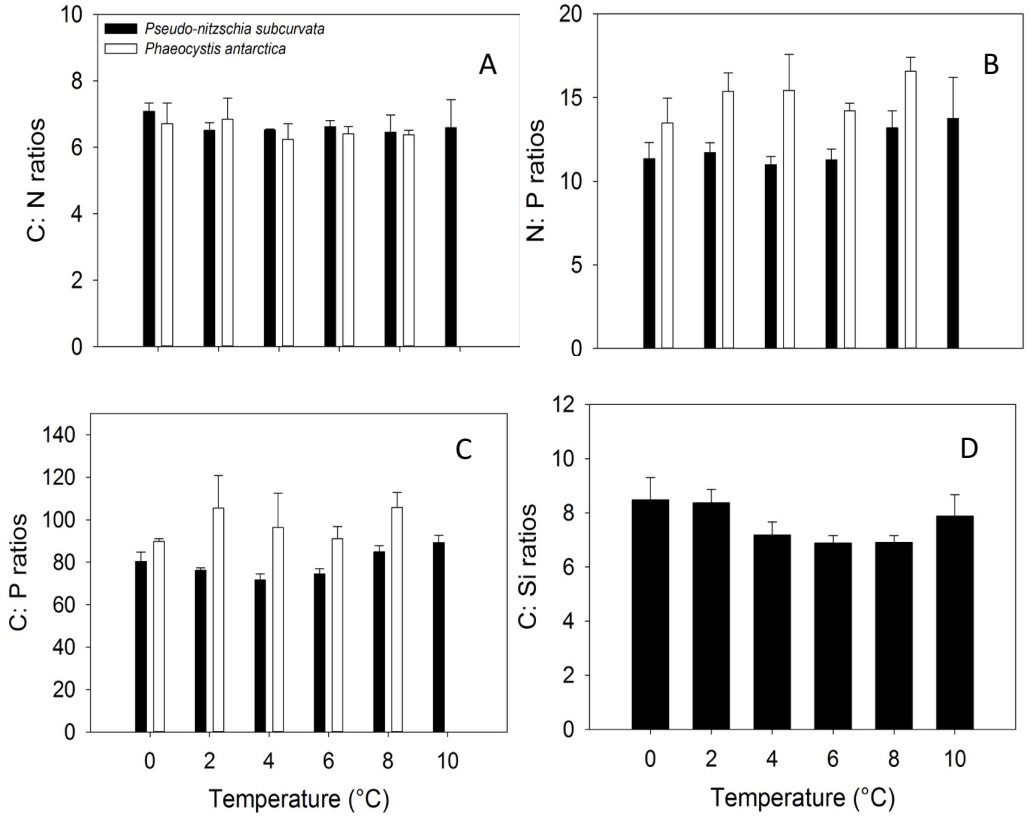

780 Fig. 3

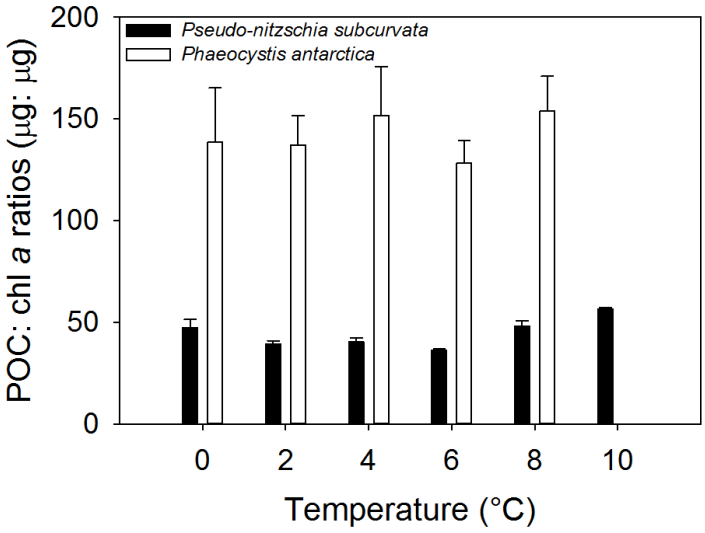
Pseudo-nitzschia subcurvata
Phaeocystis antarctica
POC: chl a ratios (μg: μg)
200
150
100
50
0
0
2
4
6
8
10
Temperature (°C)

781 Fig. 4

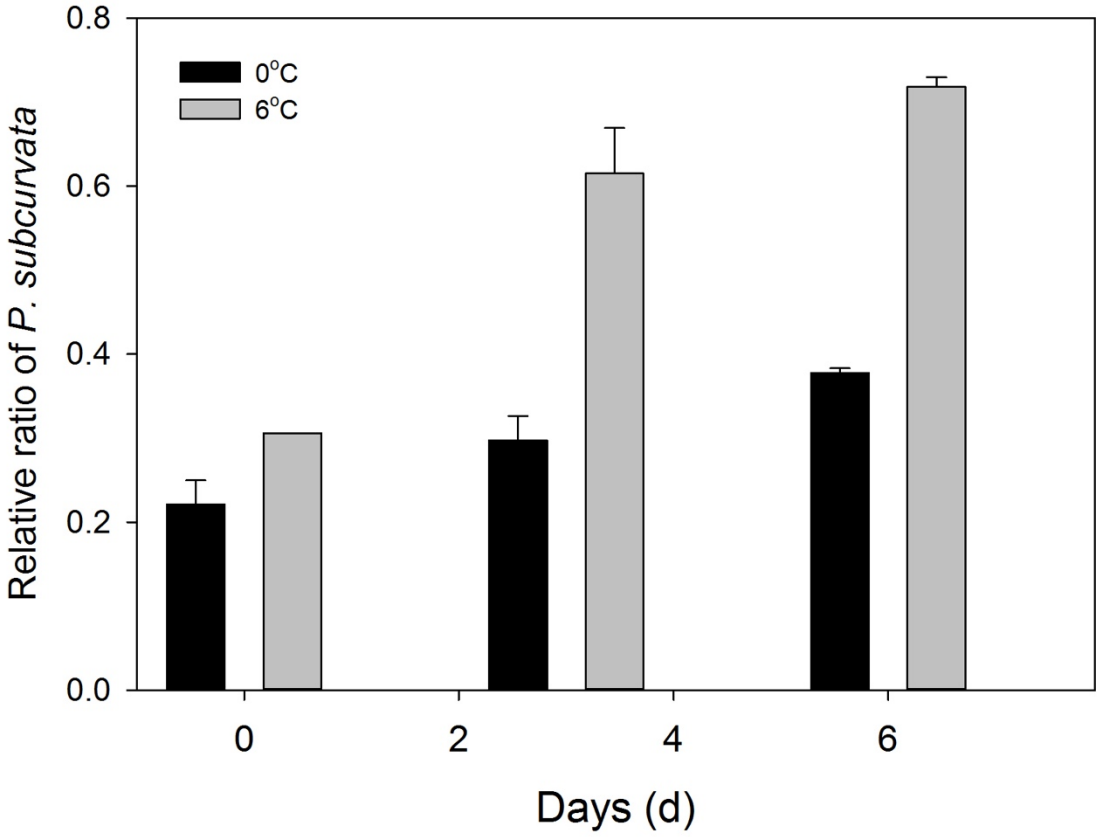

782
783

784 Fig. 5